Voltage-dependent inactivation in a cardiac-skeletal chimeric calcium channel

L. Parent*, M. Gopalakrishnan[1], A.E. Lacerda, X. Wei[2], E. Perez-Reyes[3]

Department of Molecular Physiology and Biophysics, Baylor College of Medicine, Houston, TX 77030, USA

Received 6 December 1994

Abstract **The loci for inactivation in calcium channel proteins are unknown. Mechanisms for inactivation may be distributed across Ca^{2+} channel subunits and appear to be complex, multiple and interacting. We took advantage of the properties of chimeras, constructed between cardiac (H4) and skeletal muscle (Sk4) calcium channel α_1 subunits to study the molecular mechanism of inactivation in L-type calcium channels. Sk1H3, a chimeric construct of these two L-type calcium channels, was expressed in *Xenopus* oocytes in the absence of auxiliary subunits. Sk1H3 incorporated repeat I from skeletal muscle α_1 and repeats II, III, IV from heart α_1 subunit. Sk1H3 inactivated faster ($\tau \approx 300$ ms) and more fully than the wild-type H4 with Ba^{2+} ions as the charge carrier. Thus, inactivation of Sk1H3 was 90% complete after a 5-s conditioning pulse at +20 mV while inactivation of H4 was only 37% complete. Sk1H3 inactivation also developed at more negative potentials with $E_{0.5} = -15$ mV as compared to $E_{0.5} = -5$ mV for H4. In the presence of external calcium ions, the extent of inactivation significantly increased from 37 to 83% for H4 while inactivation of Sk1H3 was only slightly increased. Inactivation with Ba^{2+} as the charge carrier was confirmed at the single- channel level where averaged single-channel ensembles showed a similar rate of inactivation. Collectively, these observations demonstrate that Sk1H3 inactivation appears to have a prominent voltage-dependent component. Whether Sk1H3 inactivation involves interactions within repeat I alone or interactions between repeat I and site(s) located in the three other repeats of the α_1 subunit has yet to be determined.**

Key words: Calcium channel; Inactivation; Chimera; Heart; Skeletal muscle; Mutagenesis

1. Introduction

Voltage-dependent calcium channels have been characterized on the basis of their electrophysiological and pharmacological properties [1]. With respect to inactivation, the T-type calcium channel is characterized by fast inactivation ($\tau < 100$ ms) while the L-type is characterized by slow inactivation ($\tau > 500$ ms). It is generally agreed that inactivation of L-type cardiac calcium channels is under the dual regulation of calcium-current dependent and voltage-dependent mechanisms [2,3], while inactivation of L-type skeletal calcium channels is primarily voltage-dependent [4]. In addition, a more fundamental question arises from the heteropentameric structure of calcium channels, namely which and to what extent each of the subunits, α_1, $\alpha_2\delta$, β, or γ is involved in the inactivation process. While the α_1 subunit determines the pore, and much of the pharmacology [48], coexpression with β subunit mRNA induces currents with faster activation and inactivation [5–7] implying that auxiliary subunits may, to varying degrees, determine activation and inactivation kinetics.

To assess the role of the α_1 subunit in determining the kinetics of calcium currents in the absence of contributions from accessory subunits, we took advantage of the properties of a chimeric calcium channel constructed from rabbit skeletal [8] and cardiac [9] muscle α_1 subunits. The construct Sk1H3, in which repeat I from the cardiac muscle α_1 subunit was replaced by repeat I from the skeletal muscle α_1 subunit, showed faster and more voltage-dependent inactivation than the cardiac muscle α_1 subunit (H4) [10]. We suggest that L-type Ca^{2+} channels contain latent sites for voltage-dependent inactivation which became functional in the Sk1H3 chimera. Whether Sk1H3 inactivation involves interactions within repeat I alone or interactions between the four repeats of the α_1 subunit has yet to be determined.

2. Methods

2.1. Construction of the skeletal-cardiac chimera

Standard methods of plasmid DNA preparation, and DNA sequencing were used [11]. A wild-type, full-length cardiac $\alpha_{1C\text{-}a}$ subunit cDNA (H4, Genbank Accession Number X15539) was cloned from rabbit [12]. The rabbit skeletal muscle α_{1S} subunit cloned (Sk4) by Perez-Reyes et al. [8] has essentially the same primary sequence as that published by Tanabe et al. [13] (Genbank Accession Number X05921). The full-length skeletal-cardiac chimeras were constructed by introducing common restriction sites in the regions of conserved sequences by polymerase chain reaction (PCR; Hoffman La Roche) mediated mutagenesis [14]. The chimera Sk1H3 was constructed by introducing the α_{1S} fragment into the $\alpha_{1C\text{-}a}$ at the site *Not*I(polylinker)/*Bam*HI (1,264). Constructs were verified by restriction mapping and the nucleotide sequence of the mutated region was determined by the dideoxy chain termination method using double-stranded plasmid DNA as previously described [9]. The deleted ΔC1733 version of Sk1H3 and the heart α_{1C} subunit, used to quantify Ca-dependent inactivation, were made according to Wei et al. [15]. The deleted form ΔC1733 construct of the wild-type heart α_{1C} subunit has been shown to generate inward barium currents 4- to 6-fold greater than the full-length wild-type α_{1C} subunit with similar macroscopic activation and inactivation kinetics (results not shown). DNA constructs were linearized at the 3′ end by *Hin*dIII digestion and run-off transcripts were prepared using methylated cap analog $m^7G(5')ppp(5')G$ and T7 RNA polymerase (Boehringer Mannheim).

2.2. Expression of α_{1C} (H4) and chimeric constructs in Xenopus oocytes

Stage V or VI individual oocytes free of follicular cells were obtained after collagenase treatment (Gibco) using published methods [16]. cRNA was injected at a concentration of 100 ng/μl (4.6 ng). Oocytes were cultured at 19°C for 3 to 7 days in a SOS solution (in mM): 100 NaCl, 2 KCl, 1.8 $CaCl_2$, 1 $MgCl_2$, 5 HEPES, 2.5 pyruvic acid, 50 μg/ml gentamicin, pH 7.6.

*Corresponding author.

[1]*Present address:* Abbott Laboratories, Pharmaceutical Products Division, Abbott Park, Il 60064-3500, USA.
[2]*Present address:* Medical College of Georgia, Inst. Molecular Medicine, Genetics Augusta, GA 30912, USA.
[3]*Present address:* Department of Physiology, Stritch School of Medicine, Loyola University, Chicago, IL 60153, USA.

SSDI 0014-5793(95)00090-9

2.3. Electrophysiological recordings

Whole-cell currents were measured at room temperature with a two-electrode voltage-clamp amplifier (OC-725, Warner Instruments). Oocytes were first impaled in a modified Ringer solution (in mM): 96 NaOH, 2 KOH, 1.8 $CaCl_2$, 1 $MgCl_2$, 10 HEPES titrated to pH 7.4 with methanesulfonic acid (MeS), then the bath solution was exchanged with the following 40 BaMeS solution (in mM): 40 $Ba(OH)_2$, 50 NaOH, 1 KOH, 0.5 niflumic acid, 0.1 EGTA, 10 HEPES titrated to pH 7.2 with methanesulfonic acid. To further minimize contamination by endogenous calcium-activated Cl^- currents, oocytes were preincubated in the presence of 100 μM Bapta-AM (Calbiochem, San Diego) for two hours. Capacitive transients and leak currents were subtracted using the residual currents measured in the presence of 1 mM $CoCl_2$.

PClamp software (Axon instruments) was used for on-line data acquisition and analysis. Pseudo h_∞ curves (steady-state inactivation) were measured using the multistep protocol illustrated in Fig. 2. The extent of steady-state inactivation was measured as the fraction of peak current during the test pulse at +30 mV relative to the peak current during the control pulse at +30 mV as a function of the interpulse potential:

$$\text{inactivation} = 1 - \frac{i_{\text{test (30 mV)}}}{i_{\text{control (30 mV)}}} \quad (1)$$

All data collected for one voltage from one frog were pooled and reported as the mean ± S.E.M. and the mean curve was then fitted to the following Boltzmann equation that accounts for the fraction of noninactivating current with $E_{0.5}$, mid-point potential; k, slope parameter; and Y_0, fraction of noninactivating current [17]:

$$Y(E_m) = 1 - \frac{1 - Y_0}{(1 + \exp(E_{0.5} - E_m)/k)} \quad (2)$$

For the activation and inactivation time constants, leak subtracted current traces were fitted using the routine provided by Clampfit (PClamp, Axon Instruments) using a correlation coefficient greater than 0.99.

Single channels were recorded in the cell-attached configuration with a Axopatch 200 A patch-clamp amplifier (Axon Instruments) after removing the vitelline membrane from the oocytes as previously described [18]. Patch pipettes were filled with a solution consisting of (in mM): 115 $BaCl_2$, 1 EGTA, 10 HEPES, pH adjusted to 7.4 with *N*-methyl-D-glucamine. Oocytes were bathed in an iso-K solution (140 K-Aspartate, 10 EGTA, 1 $MgCl_2$, 10 HEPES, pH 7.4) to cancel membrane potential. Membrane potential was thus reported directly as −(potential applied in the pipette) or $-V$pip. Single-channel conductance was measured for the full-length construct SK1H3 and H4 coinjected with auxiliary subunits α_{2b} from rat brain [45] (generously provided by Dr. Michel De Waard) and cardiac β_{2a} [20]. Single channels were recorded in the presence of 1 μM (±) Bay K 8644 (Calbiochem) in the patch pipette. Data were sampled at 5 kHz and filtered at 1.5 kHz. Single channel recordings were analyzed using PClamp software (Axon Instruments) and the TRANSIT algorithm [17].

3. Results

3.1. Comparison of Sk1H3 and H4 currents

Fig. 1 shows current traces recorded in the presence of 40 mM BaMeS for the chimeric construct Sk1H3 (bottom panel) and for the cardiac muscle α_1 subunit H4 (top panel). All wild-type and chimeric channels were tested in *Xenopus* oocytes without co-injection of auxiliary subunits. Voltage pulses were applied from −20 to +20 mV in increments of 10 mV (top to bottom). H4 yielded currents that peaked at ≈100 ms after the voltage step and did not noticeably inactivate during the 450 ms-pulse. The absence of significant Ba-inactivation has also been reported for α_{1C} alone transfected in cultured cell lines CHO [43] and HEK-293 [42]. In contrast, Sk1H3 showed noticeable inactivation with barium as the charge carrier. At +10 mV, Sk1H3 current inactivated during the voltage pulse with $\tau_{\text{inactivation}} > 1{,}000$ ms. Inactivation sped up as the depolarization steps grew larger and $\tau_{\text{inactivation}}$ decreased from 540 ms (S.E.M. = 51, n = 26) at +20 mV to 308 ms (S.E.M. = 8; n = 26) at +30 mV (not shown). The emergence of voltage-dependent inactivation suggests that the locus for voltage-dependent inactivation in L-type α_1 subunits is located in repeat I as it has been shown for non-dihydropyridine- sensitive α_1 subunits, α_{1A} and α_{1E} [33].

Current traces shown here were obtained with the full-length Sk1H3 and full-length H4 but similar results were obtained with the 3′ end deleted constructs Sk1H3ΔC1733 and H4ΔC1733 (results not shown). Analysis also revealed a single activation time constant of 12 ms for Sk1H3 as compared to $\tau_1 = 2$ and $\tau_2 = 30$ ms for H4 (Table 1). The slightly slower activation of Sk1H3 is consistent with previous reports that Repeat I of the α_1 subunit determines the activation kinetics in calcium channels [32,39]. In addition, currents generated by Sk1H3 were generally 2 to 5-fold larger than the currents generated by H4 when assayed under the same conditions (Table 1) although the wild-type skeletal muscle α_{1S} subunit does not express in oocytes [19]. The rate and the extent of the current inactivation for both channels was independent of the current density. Sk1H3 and H4 were described by similar peak current–voltage relationships with a steeper slope of activation for Sk1H3 (results not shown). As measured in the presence of 40 mM BaMES, Sk1H3 currents peaked at +30 mV (S.E.M. = 0.5, n = 32) as compared to +33 mV (S.E.M. = 1; n = 9) for H4 currents.

Despite the enhanced inactivation, whole-cell currents induced by Sk1H3 otherwise displayed features of L-type calcium currents. Sk1H3 conducted alkali divalent cations in the order $Ba^{2+} \gg Sr^{2+} > Ca^{2+}$ and Sk1H3 currents were typically stimulated 3–5-fold by the addition of 500 nM Bay K 8644 to the bath (results not shown). Furthermore, Sk1H3 expression increased and its kinetics were modulated after co-injection with the ancillary subunits α_{2b} and brain/cardiac β_{2a} subunit as it has been shown for the wild-type cardiac muscle α_1 subunit [20] (results not shown).

3.2. Voltage-dependent inactivation in Sk1H3

Oocytes were preincubated with 100 μM Bapta-AM to prevent activation of endogenous Ca-dependent Cl^- currents. This concentration was found to prevent activation of endogenous Cl^-currents without abolishing calcium-dependent inactivation in expressed α_{1C} subunits [40].

Table 1
Properties of Ba-activated currents +20 mV

RNA construct	Peak current (nA)	τ act (1) (ms)	τ act (2) (ms)	τ inactivation (ms)
H4	269 ± 20 (n = 23)	2.0 ± 0.2 (n = 18)	30 ± 4 (n = 18)	not measurable
Sk1H3	788 ± 73 (n = 26)	not measurable	11.7 ± 0.6 (n = 26)	540 ± 51 (n = 26)

Mean values ± S.E.M. for data collected in the presence of 40 mM BaMeS. Current density was reported as the peak current measured in the presence of 40 mM BaMeS. All experiments were performed 3 to 5 days after mRNA injection. Endogenous calcium currents were <20 nA under the same conditions [18]. Time constants for activation and inactivation were obtained by fitting the whole-cell current traces (after leak subtraction) for each test potential recorded during a 450 ms pulse. The first activation time constant for Sk1H3 reflects the contribution from residual capacitive transient. Inactivation of H4 was not measurable under these conditions ($\tau_{\text{inactivation}} > 5$ s).

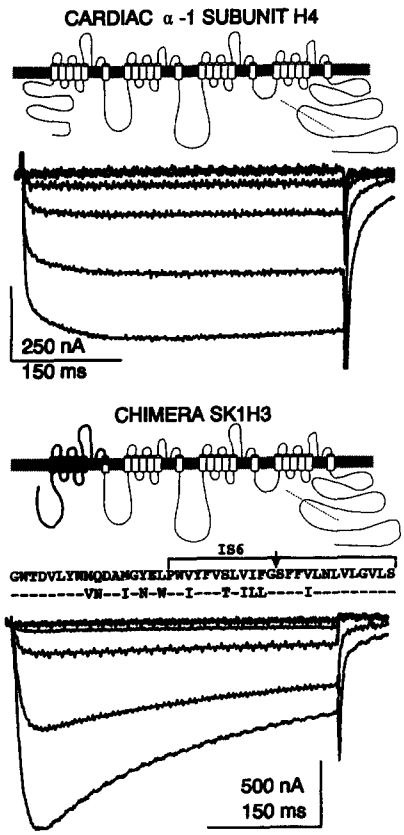

Fig. 1. Top panel: the cardiac muscle $\alpha_{1C\text{-}a}$ subunit (H4) is comprised of four proposed repeats. The dashed line at the C-terminus indicates the approximate end of the ΔC1733 version alternatively used in some experiments. Current traces obtained in 40 mM BaMeS with H4 are shown from −20 to +20 mV in 10 mV increments from a holding potential of −80 mV. Bottom panel: the chimeric construct Sk1H3 was created by exchanging most of the first repeat of the parent cardiac muscle $\alpha_{1C\text{-}a}$ subunit with the first 321 AA of the skeletal muscle α_{1S} subunit up to the middle of IS6 (filled segments). The amino acid sequences of wild-type $\alpha_{1C\text{-}a}$ (H) and wild-type α_{1S} (S) are shown in the region surrounding IS6; this region is highly conserved with only 10 substitutions between the two α_1 subunits. Sk1H3 construct was made using the unique *Bam*HI restriction site as indicated by the arrow (↓). SK1H3 current traces were recorded in the presence of 40 mM BaMeS, using 15 pulses of 450 ms duration between −30 and +40 mV (5 mV interval) from a holding potential of −80 mV. Traces obtained at −20; −10; 0; +10 to +20 mV (top to bottom) are shown here. Episodes were recorded at a frequency of 0.1 Hz and currents were filtered at 100 Hz. Scale bars are 250 nA and 150 ms (H4) and 500 nA and 150 ms (Sk1H3).

SK1H3 inactivation was quantified using the triple-pulse protocol shown on the top panel of Fig. 2. This multistep protocol was designed to offset the sizable current run-down observed during the course of a 10 min experiment. Peak current was first recorded at +30 mV before a series of 5 s depolarizing potentials was applied from −80 to +30 mV. The extent of steady-state inactivation was then measured as the fraction of the peak current recorded during the test pulse at +30 mV relative to the current measured during the first pulse at +30 mV.

Steady-state inactivation was first investigated in the presence of barium ions to characterize voltage-dependent inactivation (Fig. 2). In the presence of 40 mM BaMeS, H4 currents did not strongly inactivate during the 5 s depolarizing pulse to +20 mV as shown in the middle panel of Fig. 2. The quasi-absence of large tail currents during the repolarization step at −100 mV and at the end of the pulse protocol, suggests minimal kinetic contamination by endogenous Cl^- currents as activation of Cl^- currents was shown to cause slow tail currents of several μA in magnitude during repolarization steps. The maximum level of steady-state inactivation was 37% (S.E.M. = 2, n = 8) with a mid-point of inactivation $E_{0.5}$ at −5 mV (S.E.M. = 1, n = 8). Voltage-dependent inactivation of H4 was only partial and developed after the current activation threshold. This coupling between activation and inactivation was reminiscent of the calcium-dependent inactivation identified in native cardiac calcium currents. Indeed, inactivation of H4 was substantially increased in the presence of external calcium ions (Fig. 3, upper left panel). External calcium caused the current to inactivate faster with $\tau_{inactivation}$ = 110 ms at +20 mV as shown and a mean $\tau_{inactivation}$ = 123 ms (S.E.M. = 9; n = 4) at +30 mV. Similar inactivation time constants were reported for Ca-dependent inactivation of α_{1C} alone expressed in HEK-293 cells [42]. The faster inactivation was correlated with a significant increase in the extent of steady-state inactivation which went from 37% up to 83% (S.E.M. = 1, n = 3) at +30 mV (Fig. 3, lower left panel). These results demonstrate that α_{1C} (H4) can undergo voltage- and calcium-dependent inactivation in the absence of exogenous auxiliary subunits and supports the view that the site of inactivation is located on the α_1 subunit itself [40,41].

In contrast to H4, Sk1H3 inactivated almost completely in the presence of barium with 88% (S.E.M. = 2, n = 24) of the Sk1H3 current inactivating during a 5-s pulse at +20 mV (Fig. 2). As seen in the typical current trace, Sk1H3 Ba-currents peaked less than 50 ms after the voltage step and 85% of the current has inactivated at the end of the pulse as compared to only 30% of the H4 current. Not only did Sk1H3 inactivate to a greater extent, inactivation of Sk1H3 developed before the current activation threshold unlike H4. The mid-point of inactivation $E_{0.5}$, was −15 mV (S.E.M. = 2, n = 24) for Sk1H3 which represents a −10 mV shift when compared to H4 (Fig. 2). The extent of steady-state inactivation was very reproducible for H4 and Sk1H3. Steady-state inactivation varied from 85 to 95% (88%, S.E.M. = 2, n = 24 oocytes, 6 frog donors) for Sk1H3 and from 30 to 40% (37%, S.E.M. = 2, n = 8 oocytes, 4 frog donors) for H4. The enhanced inactivation of Sk1H3 measured in the presence of barium suggests that its inactivation is more dependent upon membrane potential than external calcium ions. To assess calcium-dependent inactivation in Sk1H3, Sk1H3 currents were recorded in the presence of 40 mM CaMeS and steady-state inactivation was measured using 5-s voltage pulses as described in Fig. 2. Actual current traces shown in Fig. 3 (right panel) were recorded at +20 mV. Sk1H3 currents inactivated faster in the presence of external calcium ($\tau_{inactivation}$ = 119 ms) than in the presence of 40 mM barium ($\tau_{inactivation}$ = 498 ms). On average, Sk1H3 currents inactivated with a $\tau_{inactivation}$ = 92 ms (S.E.M. = 3; n = 25) at +30 mV in the presence of 40 mM CaMeS. This suggests that Sk1H3 can undergo calcium-dependent inactivation as well as voltage-dependent inactivation. Moreover, H4 and Sk1H3 were both found to inactivate at the same rate in the presence of calcium ions suggesting that the site responsible for calcium-dependent inactivation in α_{1C} is not located in repeat I.

External calcium ions further increased the extent of steady-state inactivation (Fig. 3, bottom right panel). In the presence of external calcium ions, 90% to 95% (mean = 93%; S.E.M. = 2, n = 16) of the current inactivated during the 5-s pulse at +20

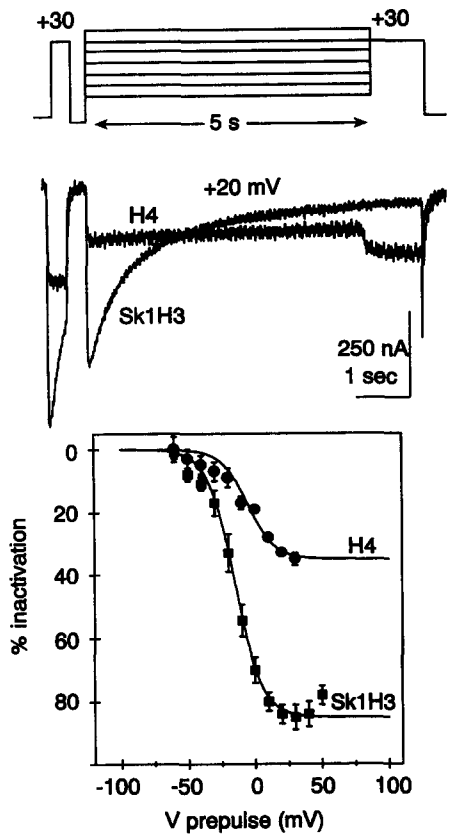

Fig. 2. Inactivation kinetics. Upper panel: measurement of the voltage-dependence of inactivation at steady-state, defined as 5 s, was complicated by a constant rundown of the whole-cell current. The multistep voltage protocol shown here was used to account for current rundown during the course of the measurement. A 250-ms control step to +30 mV (control) was first applied, followed by a 250 ms repolarization step to −100 mV before a series of 12 different 5-s interpulse potentials from −80 to +30 mV. The inactivated current was measured at +30 mV (test). Holding potential was −80 mV and episodes were applied at a frequency of 0.04 Hz. Middle panel: current traces for H4 and Sk1H3 were measured with 40 mM BaMeS at a interpulse potential of +20 mV. Note that Sk1H3 currents were initially 3 times larger than H4 currents. The current traces were digitized on-line at 150 Hz. Scale bars are 250 nA and 1 s. Lower panel: steady-state inactivation was plotted as a function of the interpulse potential. The data represent the mean values (± S.E.M.) obtained for H4 (●, $n = 4$) and for Sk1H3 (■, $n = 5$). Data are reported as the mean ± S.E.M. for each group. The data were fitted as indicated by the solid line with equation 2 (see section 2). For H4 (●), the parameters were: $k = 2.5$, $E_{0.5} = -5$ mV, $Y_0 = 0.65$ and for Sk1H3 (■), $k = 2.5$, $E_{0.5} = -15$ mV and $Y_0 = 0.15$.

mV with a mid-point of inactivation $E_{0.5} = -16$ mV (S.E.M. = 1, $n = 16$). The increase in steady-state inactivation is however barely significant since at this time scale, voltage alone had inactivated 88% of the current as seen in the presence of 40 mM BaMeS.

To characterize the effect of current density, steady-state inactivation of Sk1H3 was measured in the presence of 10 mM BaMeS (Fig. 3, right panel). A 450 ms-current trace recorded in the presence of 10 mm BaMeS is shown in Fig. 3. At +20 mV, Sk1H3 currents inactivated with $\tau_{inactivation} = 314$ ms not significantly different than the τ measured at +30 mV in the presence of 40 mM BaMeS. Sk1H3 inactivation was also similar whether measured in the presence of 10 or 40 mM BaMeS. As much as 89% (S.E.M. = 3, $n = 6$) of the current recorded in the presence of 10 mM Ba^{2+} inactivated during a 5-s pulse at +20 mV as compared to 90% in the presence of 40 mM Ba^{2+}. Inactivation developed with a mid-point of inactivation of −26 mV (S.E.M. = 1, $n = 6$) in the presence of 10 mM Ba^{2+} as compared to a mid-point of inactivation of −15 mV in the presence of 40 mM BaMeS consistent with a similar shift of −15 mV in the activation curve.

In summary, Sk1H3 inactivated more completely than H4 with ≈90% of the Ba-current inactivating during a 5-s prepulse; its inactivation developed at more negative potentials with a mid-point of inactivation $E_{0.5} = -15$ mV as compared to −5 mV for H4; and the extent of inactivation was not significantly increased by external calcium ions. Furthermore, Sk1H3 inactivation was independent of the level of expression, the current density, and individual frog variations since experiments reported here were performed in paired oocytes from the same donor. These observations collectively convey that Sk1H3 inactivation is markedly different than the inactivation of H4 with a prominent voltage-dependent component.

3.3. *Inactivation at the single-channel level*

The Ba^{2+}-inactivation kinetics of Sk1H3 recorded at the macroscopic level were reproduced at the single-channel level. Fig. 4 summarizes a series of cell-attached experiments performed with 115 mM $BaCl_2$ and in the absence of Bay K in the patch pipette. Sk1H3 channels were recorded between 0 and +60 mV and current ensembles were averaged from 30 pulses for each test potential (Fig. 4, top left panel). At +30 mV, the ensemble average of the unitary Ba^{2+} currents ($< I > = i*N*Po$) was small ($< I \gg -0.5$ pA) with no significant time-dependent decline during the 320 ms-pulse. At +60 mV, however, Sk1H3 current peaked 50 ms after the voltage step and steadily inactivated thereon. As much as 40% of the current inactivated from a peak current of −2.5 pA to −1.1 pA at the end of the pulse. This level of inactivation was equivalent to the whole-cell inactivation reported for Sk1H3 in Fig. 1 where 55% of the current declined during the 450 ms-pulse at +20 mV. In contrast, there was no measurable inactivation for H4 ensemble average current recorded under the same conditions (Fig. 4, top right panel). Although the duration of the pulses applied to H4 were shorter than for Sk1H3, there was no measurable inactivation of H4 at the end of the 160 ms pulse. Similar results were obtained when H4 and Sk1H3 were co-expressed with α_2 and β_2 subunits (results not shown). Sk1H3 was similar to H4 in its single-channel conductance (Fig. 4, bottom left panel). From the slopes of single-channel I-V curves measured between −20 and +20 mV, the single-channel conductance of Sk1H3 was estimated to be 21 pS (S.E.M. = 1; $n = 3$ oocytes) which is similar to the single-channel conductance of 22 pS (S.E.M. = 0.5; $n = 4$ oocytes) estimated for H4 under the same conditions [23–25]. Repeat I affected the calcium channel kinetics without affecting its single-channel conductance. With respect to conductance, this result supports the view that the S5-S6 linker in Repeat I does not play a prominent role in the calcium channel pore properties [29].

4. Discussion

4.1. *Expression of chimeric skeletal-cardiac* α_1 *subunits*

Expression of skeletal and cardiac muscle α_1 subunits of the L-type calcium channel have been assayed in several systems.

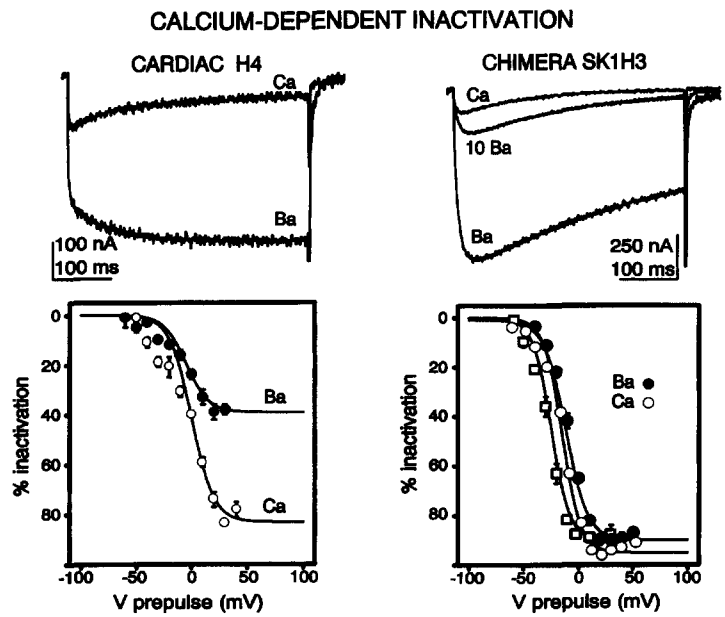

Fig. 3. Calcium-dependent inactivation. Upper left panel: H4 ΔC1733 currents were recorded in the presence of 40 mM CaMeS or 40 mM BaMeS and steady-state inactivation was measured according to the protocol described earlier. Typical 450 ms-current traces obtained from 2 different oocytes are shown at +20 mV. The small tail current in the presence of external calcium ions suggests minimum contamination by endogenous Ca^{2+}-activated Cl^- current. External calcium caused the current to inactivate faster with a single $\tau_{inactivation}$ = 100 ms and a mean $\tau_{inactivation}$ = 123 ms (S.E.M. = 9; n = 4) at +30 mV. Barium current traces were fitted with a sum of 2 activation time constants τ_1 = 3 ms and τ_2 = 67 ms with no measurable inactivation. Lower left panel: in the presence of external calcium (○), 83% (S.E.M. = 1, n = 3) of the current inactivated during a 5-s pulse at +20 mV as compared to only 37% (S.E.M. = 2, n = 4) in the presence of barium (●). Solid lines show the fits of the mean data to the modified Boltzmann equation (eq. 2) with $E_{0.5}$ = −5 mV, k = 2.5, Y_0 = 0.65 (40 mM Ba^{2+}) and $E_{0.5}$ = 0 mV, k = 2.5, Y_0 = 0.2 (40 mM Ca^{2+}). Upper right panel: Sk1H3 ΔC1733 currents were recorded using 450 ms-pulses in the presence of 40 mM CaMeS, 10 mM BaMeS, 40 mM BaMeS (top to bottom) at a membrane potential of +20 mV on 3 different oocytes. Scale bars are 250 nA and 100 ms. Current traces were fitted to a sum of 2 exponential functions with τ_{act} = and τ_{inact} = 119 ms (40 Ca); τ_{act} = 10 ms and τ_{inact} = 314 ms (10 Ba); τ_{act} = 9 ms and τ_{inact} = 498 ms (40 Ba). Lower right panel: steady-state inactivation was measured in the presence of 40 mM BaMeS (●, n = 6); 40 mM CaMeS (○, n = 8) and 10 mM BaMeS (□, n = 3) and reported as a function of the 5-s interpulse potential. Solid lines show the fits to the Boltzmann equation (eq. 2) with the following parameters: 40 mM BaMeS ($E_{0.5}$ = −12 mV; k = 2.5, Y_0 = 0.10); 40 mM CaMeS ($E_{0.5}$ = −15 mV, k = 3, Y_0 = 0.05); 10 mM BaMeS ($E_{0.5}$ = −25 mV; k = 2.8; Y_0 = 0.10).

Injection of cRNA encoding the cardiac muscle α_1 subunit produced calcium currents in *Xenopus laevis* oocytes [12,26], but injection of cRNA encoding the skeletal muscle α_1 subunit failed to elicit calcium currents [19]. The skeletal α_1 subunit was expressed in mouse dysgenic myotubes [27] and mouse L cells where it was shown to express currents in the absence of other endogenous calcium channel subunits [5,8]. However, the levels of current expressed in murine L cells was very low (0.57 pA/pF) and even lower for the cardiac α_1 subunit (0.02 pA/pF) [28]. For dysgenic myotubes, expression turned out to be higher for the cardiac muscle α_1 subunit with an estimated current density of 28 pA/pF as compared to 4 pA/pF for the skeletal muscle α_1 subunit [27].

4.2. *Calcium-dependent inactivation in the cardiac α_1 subunit*

The results of the present study indicate that the cloned heart α_{1C} subunit alone expressed in *Xenopus* oocytes undergoes calcium- and voltage-dependent inactivation. Calcium-dependent inactivation can be measured successfully after eliminating endogenous Ca^{2+}-dependent Cl^- currents by preincubation with 100 μM Bapta-AM combined with complete replacement of Cl^- ions. In a different study, calcium-dependent inactivation of α_{1C} alone was also successfully measured in *Xenopus* oocytes after intracellular injection of 1 to 50 mM Bapta [40]. The rate of calcium-dependent inactivation reported herein is similar than that reported for α_{1C} alone expressed in mammalian CHO cells [41] and HEK-293 cells [42] which further supports the view that calcium-dependent inactivation is an intrinsic property of the α_1 subunit [40] and is independent of the expression system.

The rate of calcium-dependent inactivation for expressed α_{1C} alone is however significantly slower than that reported for native calcium channels in cardiac cells of frog and mammalian preparations [2,3,46]. Ancillary subunits such as β and α_2 may be required to achieve the rate of calcium channel inactivation measured in native cells. It is now universally recognized that co-expression of β subunit mRNA induces barium currents with faster activation and inactivation kinetics [5–7,25,33,35]. β subunits were found to increase the rate of voltage-dependent inactivation when co-expressed with α_{1A}, α_{1C}, and α_{1E} subunits with $\beta_3 > \beta_1 > \beta_2$ in decreasing order of influence [25,33,35,44]. Co-expression with β_1 subunit was lately shown to speed up calcium-dependent inactivation for $\alpha_{1C\text{-}b}$ stably expressed in CHO cells [43] and for $\alpha_{1C\text{-}a}$ transiently expressed in HEK-293 cells [42], by introducing a second and faster inactivation time constant $\tau_f \approx 30$–40 ms. Co-expression of α_{1C}/β_1 with α_2 subunit further increased calcium-dependent inactivation with τ_f going from 38 to 20 ms [43] suggesting that the multisubunit complex $\alpha_1/\beta/\alpha_2$ is necessary to fully reproduce native calcium-dependent inactivation [42].

Sk1H3 was also shown to undergo calcium-dependent inactivation. In fact, H4 and Sk1H3 were found to inactivate at the

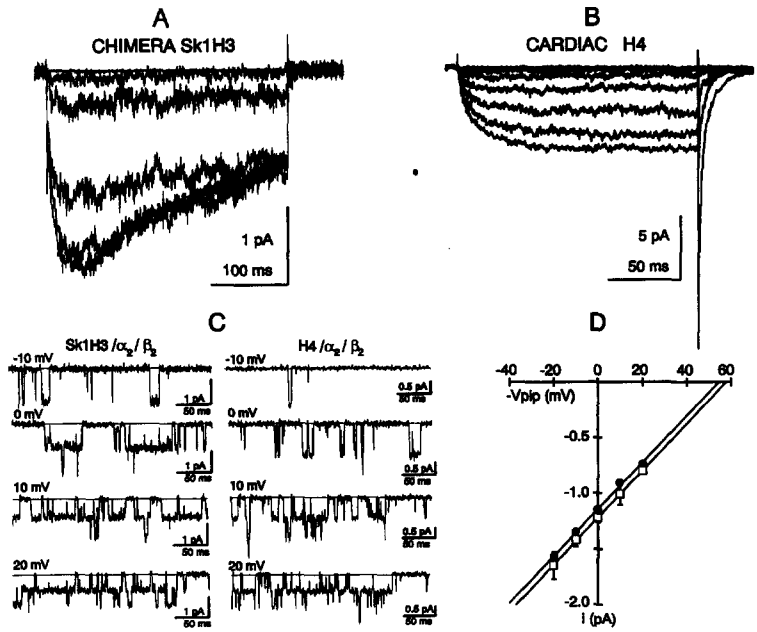

Fig. 4. Inactivation of full-length Sk1H3 and H4 single-channels. Upper panel: ensemble-averaged Ba^{2+} currents obtained from cell-attached patches in the presence of 115 mM $BaCl_2$ for the chimera Sk1H3 (left panel) and H4 (α_{1C}) (right panel). Upper left panel: for Sk1H3, single channels were averaged for 30 episodes of 320 ms for voltages of 0, +10, +20, +30 ,+40 ,+50 and +60 mV (top to bottom) from a holding potential of −40 mV. Current reverses at +60 mV. Pulses were applied at a frequency of 0.5 Hz and each episode was analog filtered at 1 kHz (−3 dB). Current ensembles were corrected for leak current by subtracting and scaling null current traces obtained in the same patch from a holding potential of 0 mV. Upper right panel: for H4, single-channels were recorded from a holding potential of −60 mV at voltages of −20, −10, 0, +10, +20, +30, +40, +50 mV (top to bottom). 19 episodes of 160 ms were recorded at a frequency of 2 kHz. Lower left panel: single channels from Sk1H3/α_2/β_2 and H4/α_2/β_2 were obtained in the cell-attached configuration in the presence of 1 μM Bay K and 115 mM $BaCl_2$ as the charge carrier. For each trace, patch membrane was pulsed for 320 ms to the membrane potential as indicated from a holding potential of −40 mV. There were at least 3 independent channels in each experiment. Channel openings are downward and the closed state is indicated by the straight line. Lower right panel: comparison of the single-channel conductance of H4 (□) and Sk1H3 (●). Data points are shown as the mean ± S.E.M. of the single-channel amplitude as a function of the membrane potential from 3 oocytes for SK1H3 and 4 oocytes for H4. The average single-channel conductance was estimated by fitting data with a linear regression and averaging the least square slope values. As measured between −20 and +20 mV, the slope conductance was 21 pS (S.E.M. = 1; n = 3 oocytes) for Sk1H3 and was 22 pS (S.E.M. = 0.5; n = 4 oocytes) for H4.

same rate in the presence of calcium ions (40 mM CaMeS) suggesting that the site responsible for calcium-dependent inactivation in α_{1C} is preserved in the chimera Sk1H3. This observation is consistent with the recent report that calcium-dependent inactivation is otherwise abolished when the cardiac α_{1C} cytoplasmic linkers are replaced by their skeletal muscle α_{1S} counterparts [42]. Together, these results suggest that calcium- and voltage-dependent inactivation are controlled by distinct sites on the α_1 subunit of the cardiac L-type calcium channel.

4.3. Locus of voltage-dependent inactivation in calcium channels

Alpha-1 (α_1) subunits from rapidly inactivating neuronal calcium channels have been cloned and functionally expressed in oocytes [25,34–37]. All these α_1 subunits showed rapid inactivation in the presence of barium as the charge carrier but, with the exception of the low voltage-activated rat α_{1E} subunit [37], none has been expressed in the absence of auxiliary subunits. Thus, the question of whether voltage-dependent inactivation absolutely required interaction of α_1 with β subunits has scarcely been addressed before. Herein, we have shown that β subunits are not obligatory for voltage-dependent inactivation of calcium channels, and that inactivation is an intrinsic property of the α_1 subunit.

The skeletal-cardiac chimeric construct, Sk1H3, showed prominent inactivation in the presence of external barium, a feature that was absent in the wild-type cardiac muscle α_1 subunit. More importantly, the fast inactivation kinetics were observed in the absence of co-expressed β subunits. Although fast inactivation properties were unanticipated, the critical role of repeat I in L-type calcium channel function has been demonstrated before. Repeat I was shown to be the major determinant of the L-type calcium current activation kinetics [32,39]. The emergence of voltage-dependent inactivation in Sk1H3 suggests that the locus for voltage-dependent inactivation in L-type α_1 subunits might be located in repeat I as it has been shown for the dihydropyridine insensitive α_{1E} subunit [33]. In this last study, a stretch of ≈200 residues that encompasses IS6 and includes the site of interaction for β subunits in the I-II cytoplasmic linker [47], was shown to confer voltage-dependent inactivation when transferred from α_{1E} to α_{1A} [33]. This region is shown above with the corresponding amino acid sequence for the rabbit α_{1A} (bii2) [34]; the cardiac α_{1C} (H4) [26]; the skeletal muscle α_{1S} (Sk) [27]; the chimera Sk1H3; the marine doe-1 α_{1E} (Do) [35]; and the rat α_{1E} (Rt) [37] (Scheme 1).

```
          319                  ┌──────IS6──────┐
A [Bi]: GWTDLLYNSNDASGNTWNWLYFIPLIIIGSFFMLNLVLGVLSGEFAKERERVENRRAFLK
C [H4]: ----V--WMQ--M-YELP-V--VS-V-F----V-----------S----KAKA-GD-Q-
S [Sk]: ----V--WV---I--E-P-I--VT--LL----I-----------T----KAKS-GT-Q-
Sk1H3 : ----V--WV---I--E-P-I--VT--LL----V-----------S----KAKA-GD-Q-
E [Do]: ---TI---TD--L-AM---------------V----------------------S---
E [Rt]: ---TV---T---L-AT---------------V----------------------M-
```

Scheme 1.

As seen, there are 9 non-conserved amino acids between α_{1A} and doe-1 α_{1E} (TI..TD..L.AM..V..S). Within these residues, the

double point mutation $^{351}M \rightarrow V + {}^{375}A \rightarrow S$ (shown in bold letters) was found the most effective into conferring fast inactivation to α_{1A} [33]. Mutations at these positions cannot however account for our results since all residues are strictly conserved between Sk1H3 and α_{1C} from the *Bam*HI site in the middle of IS6 down to the C-terminus. Moreover, calcium channel inactivation is reasonably more complex, for identical residues produce opposite inactivating phenotype in different α_1 subunits. For instance, H4 (α_{1C}) possesses a valine residue aligned with M351 but does not show fast barium inactivation of doe-1 α_{1E}. On the other hand, the fast-inactivating rat α_{1E} [37] has a alanine residue that correspond to the A375 residue found in the slow inactivating α_{1A}.

Observations gathered with cardiac-skeletal chimeras and α_{1A}-doe1 chimeras [33] together point toward repeat I and more specifically IS6 [33] as the molecular determinant of voltage-dependent inactivation in calcium channel α_1 subunits. At this time, it is not known yet whether repeat I contributes the inactivation gate or the receptor site for a putative inactivation ball. Similarly, it remains to be determined whether calcium channel inactivation involves interactions within repeat I alone or interactions between the four repeats of the α_1 subunit.

Acknowledgements: We thank Dr. Michel De Waard for the rat brain α_{2b} subunit; Wei-Qiang Dong and Raynard Cockrell for oocyte handling; Tyrone Rodriguez, Sharon Chang and Cheng-Di Zuo for technical help; and Dr. A.M. Brown for support and encouragement. This work was supported by NIH Grant HL37044 to A.M.B. and AHA-TX Grant 94G-195 to L.P.

References

[1] Hille, B. (1992) Ionic channels of excitable membranes, Sinauer, Sunderland, MA.
[2] Kass, R.S. and Sanguinetti, M.C. (1984) J. Gen. Physiol. 84, 705–726.
[3] Lee, K.S., Marban, E. and Tsien, R.W. (1985) J. Physiol. 334, 395–411.
[4] Cota, G. and Stefani, E. (1989) J. Gen. Physiol. 94, 937–951.
[5] Lacerda, A.E., Kim, H.S., Ruth, P., Perez-Reyes, E., Flockerzi, V., Hofmann, F., Birnbaumer, L. and Brown, A.M. (1991) Nature 352, 527–530.
[6] Varadi, G., Lory, P., Schultz, D., Varadi, M. and Schwartz, A. (1991) Nature 352, 159–162.
[7] Singer, D., Biel, M., Lotan, I., Flockerzi, V., Hofman, F. and Dascal, N. (1991) Science 253, 1553–1557.
[8] Perez-Reyes, E., Kim, H.S., Lacerda, A.E., Horne, W., Wei, X., Rampe, D., Campbell, K.P., Brown, A.M. and Birnbaumer, L. (1989) Nature 340, 233–236.
[9] Perez-Reyes, E., Wei, X., Castellano, A. and Birnbaumer, L., (1990) J. Biol. Chem. 265, 20430–20436.
[10] Parent, L., Gopalakrishnan, M., Lacerda, A.E. and Brown, A.M. (1994) Biophys. J. 66 (abstract) A230.
[11] Sambrook J., Fritsch, E.F. and Maniatis, T. (1989) Molecular Cloning, A Laboratory Manual, Cold Spring Harbor Laboratory, Cold Spring Harbor, New-York.
[12] Wei, X., Perez-Reyes, E., Lacerda, A.E., Schuster, G., Brown, A.M. and Birnbaumer, L. (1991) J. Biol. Chem. 266, 21943–21947.
[13] Tanabe, T., Takeshima, H., Mikami, A., Flockerzi, V., Takahashi, H., Kangawa, K., Kojima, M., Matsuo, H., Hirose, T. and Numa, S.S, (1987) Nature 328, 313–318.
[14] Ho, S.N., Hunt, H.D., Horton, R.M., Pullen, J.K. and Pease, L.R. (1989) Gene 77, 51–59.
[15] Wei, X., Neely, A., Lacerda, A.E., Olcese, R., Stefani, E., Perez-Reyes, E. and Birnbaumer, L. (1994) J. Biol. Chem. 269, 1635–1640.
[16] Goldin, A.L. (1992) in: Methods in Enzymology (Rudy, B. and Iverson, L.E. Eds.) Ion Channels, Vol. 207, pp. 266–279, Academic Press, San Diego.
[17] VanDongen, A.M.J., Frech, G.C., Drewe, J.A., Joho, R.H. and Brown, A.M. (1990) Neuron 5, 433–443.
[18] Lacerda, A.E., Perez-Reyes, E., Wei, X., Castellano, A., Birnbaumer, L. and Brown, A.M. (1994) Biophys. J. 66, 1833–1843.
[19] Dascal., N., Lotan, I., Karni, E. and Gigi, A. (1992) J. Physiol. 450, 469–490.
[20] Perez-Reyes, E., Castellano, A., Kim, H.S., Bertrand, P., Baggstrom, E., Lacerda, A.E., Wei, X. and Birnbaumer, L. (1992) J. Biol. Chem. 267, 1792–1797.
[21] Ma, J. and Coronado, R. (1988) Biophys. J. 53, 387–395.
[22] Mejía-Alvarez, R., Fill, M. and Stefani, E. (1991) J. Gen. Physiol. 97, 393–412.
[23] Rosenberg, R.L., Hess, P. and Tsien, R.W. (1988) J. Gen. Physiol. 92, 27–54.
[24] Tsien, R.W., Lipscombe, D., Madison, D.V., Bley, K.R. and Fox, A.P. (1988) Trends Neurol. Sci. 11, 431–437.
[25] Sather, W.A., Tanabe, T., Zhang, J.-F., Mori, Y., Adams, M.E. and Tsien, R.W. (1993) Neuron 11, 291–303.
[26] Mikami, A., Imoto, K., Tanabe, T., Niidome, T., Mori, Y., Takeshima, H., Narumiya, S. and Numa, S. (1989) Nature 340, 230–233.
[27] Tanabe, T., Mikami, A., Numa, S. and Beam, K.G (1990) Nature 344, 451–453.
[28] Lory, P., Varadi, G., Slish, D.F., Varadi, M. and Schwartz, A. (1993) FEBS Lett. 315, 167–175.
[29] Yang, J., Ellinor, P.T., Sather, W.A., Zhang, J.F. and Tsien, R.W. (1993) Nature 366, 158–161.
[30] Almers, W., Fink, R. and Palade, P.T. (1981) J. Physiol. 312, 177–207.
[31] Beam, K.G. and Knudson, C.M. (1988) J. Gen. Physiol. 91, 781–798.
[32] Tanabe, T., Adams, B.A., Numa, S. and Beam, K.G. (1991) Nature 352, 800–803.
[33] Zhang, J.F., Ellinor, P.T., Aldrich, R.W. and Tsien, R.W. (1994) Nature 372, 97–100.
[34] Mori, Y., Friedrich, T., Kim, M.-S., Mikami, A., Nakai, J., Ruth, P., Bosse, E., Hofmann, F., Flockerzi, V., Furuichi, T., Mikoshiba, K., Tanabe, T. and Numa, S. (1991) Nature 350, 398–402.
[35] Ellinor, P., Zhang, J.-F., Randall, A.D., Zhou, M., Schwarz, T.L., Tsien, R.W. and Horne, W.A. (1993) Nature 363, 455–458.
[36] Fujita, Y., Mynlieff, M., Dirksen, R.T., Kim, M.-S., Niidome, T., Nakai, J., Friedrich, T., Iwabe, N., Miyata, T., Furuichi, T., Furutama, D., Mikoshiba, K., Mori, Y. and Beam, K.G. (1993) Neuron 10, 585–598.
[37] Soong, T.W., Stea, A., Hodson, C.D., Dubel, S.J., Vincent, S.R. and Snutch, T.P. (1993) Science 260, 1133–1136.
[38] Hoshi, T., Zagotta, W.N. and Aldrich, R.W. (1990) Science 250, 533–538.
[39] Nakai, J., Adams, B.A., Imoto, K. and Beam, K.G. (1994) PNAS 91, 1014–1018.
[40] Neely, A., Olcese, R., Wei, X., Birnbaumer, L. and Stefani, E. (1994) Biophys. J. 66, 1895–1903.
[41] Welling, A., Kwan, Y.W., Bosse, E., Flockerzi, V., Hofmann, F., Kass, R.S. (1993) Circ. Res. 73, 974–980.
[42] Zong, S., Zhou, J. and Tanabe, T. (1994) Biochem. Biophys. Res. Comm. 201, 1117–1123.
[43] Welling, A., Bosse, E., Cavalié, A., Bottlender, R., Ludwig, A., Nastainczyk, W., Flockerzi, V. and Hofmann, F. (1993) J. Physiol. 471, 749–765.
[44] Hullin, R., Singer-Lahat, D., Freichel, M., Biel, M., Dascal, N. Hofmann, F. and Flockerzi, V. (1992) EMBO J. 11, 885–890.
[45] Williams, M.E., Feldman, D.H., McCue, A.F., Brenner, R., Velicelebi, G., Ellis, S.B. and Harpold, M.M. (1992) Neuron 8, 71–84.
[46] Campbell, D.L., Giles, W.R., Hume, J.R. and Shibata, E.F. (1988) J. Physiol. 403, 287–315.
[47] Pragnell, M., De Waard, M., Mori, Y., Tanabe, T., Snutch, T.P. and Campbell, K.P. (1994) Nature 368, 67–70.
[48] Isom, L.L., De Jongh, K.S. and Catterall, W.A. (1994) Neuron 12, 1123–1194.